

# Optimizing the CO<sub>2</sub>- Laser Parameters to Attain the Minimum Wear Rate in Cobalt Based Hardfaced Surfaces

A. Umesh Bala<sup>\*1</sup>, Dr. R. Varahamoorthi<sup>2</sup>

<sup>1</sup>Research Scholar, Department of Manufacturing Engineering, Annamalai University, Tamil Nadu, India

<sup>2</sup>Associate Professor, Department of Manufacturing Engineering, Annamalai University, Tamil Nadu, India

## ABSTRACT

The laser hardfacing is carried out by CO<sub>2</sub> laser. AISI 304 stainless steel is used as the base metal and Stellite- 6 cobalt based powder is used as hardfaced material. In this Investigation an attempt has be made to optimizing the process parameters of laser hardfaced surfaces such as Laser Power (P), Travel Speed (T), Defocusing Distance (D) and Powder feed rate (F). The influence of the processing variables on wear rate is discussed. The experiments were conducted using design matrix based on a four factor and five level central composite rotatable design. An empirical relationship was developed to predict the Wear Rate of Cobalt-based (Stellite-6) hardfaced layer using Response Surface Methodology (RSM) technique. The optimized parameters and the influenced parameter were identified. The interaction effects of input process parameters of laser hardfacing were discussed.

**Keywords:** *Optimizing, RSM, Stellite-6, Laser Hardfacing, Wear Rate, AISI 304 SS.*

## I. INTRODUCTION

The laser hardfacing technique offers unique advantages over other processes in that the overlay or substrate hardfacing provides a metallurgical bond which is not susceptible to spallation and can easily be applied free of porosity and other defects. The process is also extremely versatile as a large variety of materials can be deposited for protection against degradation. The materials used for hardfacing should have melting point close to or lower than the substrate materials. During hardfacing, the temperature of the coating material is increased to the melting point and then allowed to solidify on the substrate. The effectiveness of hardfacing depends on the process of application of the hardfaced layer and the composition of the layer. The process should be optimized to have high deposition rate, high thermal efficiency, excellent dilution, excellent control of composition and hardfacing thickness. These processes can be grouped as torch processes, arc hardfacing process and high energy beam processes. Among high energy beam processes, laser hardfacing and electron beam hardfacing are more important. In this investigation the high energy CO<sub>2</sub> laser beam is used. The laser based techniques offer several distinct advantages over other conventional

surface modification processes. All variants of laser surface modification are characterized by very fast heating and cooling rates resulting in a rapidly solidified layer, in which both the microstructure and the distribution of the alloying elements could be tailored as required by suitably controlling the operating parameters. The metastable and non-equilibrium phases that can form as a consequence of rapid quenching, offer the possibility to develop layers with novel microstructures and properties superior to those of traditional processes.

**Table 1:** Chemical composition (wt.%) of Base material (AISI 304 SS).

C	Mn	Ni	Si	P	S	Cr	Fe
≤0.12	≤ 2.0	8.00 – 11.00	≤1.0	≤0.035	≤0.03	17.00 – 19.00	Balance

AISI 304 Stainless Steel is the most widely used variety of hardfacing materials. This steel contains Mn and C. The steel can retain completely austenitic microstructure on cooling. This material is extremely tough, wear and shock resistance and it is sensitive to plastic deformation. The increases in the work hardening rate of the steel turn the increases in the wear resistance.

This plasticity helps in dissipating energy, and in the process cracking and spalling of the hardfacing is avoided. However, there are some inherent problems associated with this material. Annealing or slow heating followed by cooling results in embrittlement of the material due to precipitation of carbides in the grain boundary. This material with high work hardening capability and moderate yield strength is capable of responding plastically to abrasion and impact loading.

Cr	C	W	Mo	Ni	Si	Fe	Mn	S	Co
28.5	1.12	5.06	0.35	1.34	1.13	0.99	0.4	0.01	Balance

**Table 2:** Chemical composition (wt.%) of Powder material (Stellite-6).

The main advantage of Cobalt based (Stellite-6) hardfacing alloys are excellent wear resistance, corrosion and oxidation resistance and that is why they are successful in replacing Iron based alloys. These alloys are however more expensive than other variety of alloys. The Cobalt-based hardfacing alloy was developed as Stellite. Stellite-6 alloys contain varying amount of Carbon, Tungsten and Molybdenum to enhance the properties. The cobalt alloy is also strengthened by chromium. The wear resistance is governed by formation of carbide, their volume fraction and size and distribution.

### 2.1 Identify The Important Process Variables and Its Limits:

Parameters	Units	Notations	Levels				
			-2	-1	0	1	2
Laser Power	W	P	2200	2400	2600	2800	3000
Travel Speed	mm/min	T	400	500	600	700	800
Defocusing Distance	mm	D	16	18	20	22	24
Powder Feed Rate	g/min	F	4	8	12	16	20

**Table 3:** Laser hardfacing parameters and their limits

The trial experiments were conducted and the working range was decided based on the quality appearance and the absence of any visible defects. Different combinations of parameters were used to carry out the trial experiments. This was done by varying any one of the factors from minimum to maximum while keeping the other parameters at constant. The working limits of the individual parameters were identified by macro and

## II. EXPERIMENTAL WORK

The Identified input parameters are Laser Power (P), Travel Speed (T), Defocusing Distance (D) and Powder Feed Rate (F). The upper limit was coded as +2 and the lower limit as -2 by using the input parameters and their working range. The design matrix was developed and the experiment were conducted as per the design matrix. The laser hardfacing parameters and their limits are tabulated in Table 3 The experimental runs were carried out based on trials AISI 304 stainless steel plate using Stellite-6 alloy to find out the feasible working limits of laser hardfacing parameters.

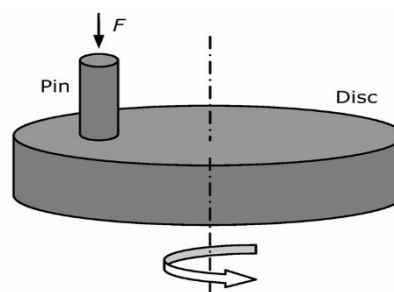


**Figure 1 :** Pin on Disc set up

micro structure. Laser hardfaced deposit which was exposed to a smooth appearance without any visible micro level defects such as crack, pores were chosen as the feasible working limits. The laser hardfacing is carried out on AISI 304 stainless steel by using CO<sub>2</sub> laser with a maximum capacity of 4000 W as per the design matrix at random order. The average deposited thickness was about 0.8–1.6 mm of the stainless steel.

After hardfacing the deposit was cut into small samples by using Electrical Discharge Machining (EDM) for wear test on pin on disc machine as shown in Figure 2. and scanned electron microscopy (SEM) images. The evaluating of wear rate for 30 samples as per the design

matrix was calculated by maintaining the wear testing parameters as constant. and the subsequent values are noted. The same wear rate values are used for deriving the empirical relationship.

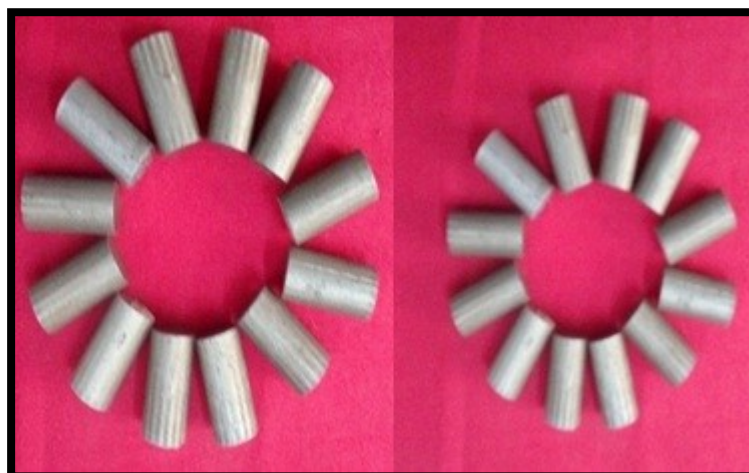


**Figure 2:** Laser Hardfaced Samples for wear test

Source	Sum of Squares	Degree of freedom	Mean Square	F-value	p-value	Significant (or) Not significant	
Model	0.0212	14	0.0015	73.01	< 0.0001	Significant	
P	0.0006	1	0.0006	28.42	< 0.0001		
T	0.0010	1	0.0010	49.09	< 0.0001		
D	0.0010	1	0.0010	49.72	< 0.0001		
F	0.0030	1	0.0030	146.52	< 0.0001		
PT	0.0001	1	0.0001	2.50	0.1349		
PD	0.0002	1	0.0002	9.71	0.0071		
PF	0.0001	1	0.0001	6.71	0.0205		
TD	0.0001	1	0.0001	4.53	0.0503		
TF	0.0003	1	0.0003	15.61	0.0013		
DF	0.0004	1	0.0004	21.44	0.0003		
P <sup>2</sup>	0.0079	1	0.0079	381.51	< 0.0001		
T <sup>2</sup>	0.0041	1	0.0041	195.22	< 0.0001		
D <sup>2</sup>	0.0000	1	0.0000	1.73	0.2084		
F <sup>2</sup>	0.0057	1	0.0057	275.61	< 0.0001		
Residual	0.0003	15	0.0000				Not Significant
Lack of Fit	0.0002	10	0.0000	0.7200	0.6928		
Pure Error	0.0001	5	0.0000				
Cor Total	0.0215	29					
R <sup>2</sup>	0.9855						
Adjusted R <sup>2</sup>	0.9720		Std. Dev.	0.0046			
Predicted R <sup>2</sup>	0.9423		Mean	0.1986			
Adeq Precision	29.3675		C.V. %	2.29			

**Table 4:** Anova Test Results

## 2.2 Experimental Design Matrix:

S.No	Coded Value				Actual Value			
	Laser Power (W)	Travel Speed (mm/min)	Defocusing Distance (mm)	Powder Feed Rate (g/min)	Laser Power (W)	Travel Speed (mm/min)	Defocusing Distance (mm)	Powder Feed Rate (g/min)
1	-1	-1	-1	-1	2400	500	18	8
2	1	-1	-1	-1	2800	500	18	8
3	-1	1	-1	-1	2400	700	18	8
4	1	1	-1	-1	2800	700	18	8
5	-1	-1	1	-1	2400	500	22	8
6	1	-1	1	-1	2800	500	22	8
7	-1	1	1	-1	2400	700	22	8
8	1	1	1	-1	2800	700	22	8
9	-1	-1	-1	1	2400	500	18	16
10	1	-1	-1	1	2800	500	18	16
11	-1	1	-1	1	2400	700	18	16
12	1	1	-1	1	2800	700	18	16
13	-1	-1	1	1	2400	500	22	16
14	1	-1	1	1	2800	500	22	16
15	-1	1	1	1	2400	700	22	16
16	1	1	1	1	2800	700	22	16
17	-2	0	0	0	2200	600	20	12
18	2	0	0	0	3000	600	20	12
19	0	-2	0	0	2600	400	20	12
20	0	2	0	0	2600	800	20	12
21	0	0	-2	0	2600	600	16	12
22	0	0	2	0	2600	600	24	12
23	0	0	0	-2	2600	600	20	4
24	0	0	0	2	2600	600	20	20
25	0	0	0	0	2600	600	20	12
26	0	0	0	0	2600	600	20	12
27	0	0	0	0	2600	600	20	12
28	0	0	0	0	2600	600	20	12
29	0	0	0	0	2600	600	20	12
30	0	0	0	0	2600	600	20	12

**Table 5:** Experimental Design Matrix and its actual values



**Figure 3:** Pin on Disc wear test machine

### III. DEVELOPING AN EMPIRICAL RELATIONSHIP

Wear rate of hardfaced surface is a function of the Laser parameters such as Laser power (P), Travel speed (T), Defocusing distance (D), Powder feed rate (F), and it can be expressed as

$$\text{Wear Rate of deposit} = f(P, T, D, F)$$

The second-order polynomial equation used to predict the response surface Y is given by

$$Y = b_0 + \sum b_i x_i + \sum b_{ii} x_i^2 + \sum b_{ij} x_i x_j$$

And for four factor, the selected polynomial could be expressed equally

$$\text{Wear Rate} = b_0 + b_1(P) + b_2(T) + b_3(D) + b_4(F) + b_{12}(PT) + b_{13}(PD) + b_{14}(PF) + b_{23}(TD) + b_{24}(TF) + b_{34}(DF) + b_{11}(P^2) + b_{22}(T^2) + b_{33}(D^2) + b_{44}(F^2)$$

where,  $b_0$  is the average of response and  $b_1, b_2, b_3, \dots, b_4$  are regression co-efficient that depends on respective linear, interactions and square terms of factors. The value of co-efficient was calculated using Design Expert software at 95% confidence level. The significance of the each co-efficient was calculated from t-test and p values. The value of "Probe > F" is less than 0.05, indicates that model terms are significant.

$$\text{Wear Rate} = \{+4.4495 - 0.0024 P - 0.0011 T - 0.0384 D - 0.0540 F - 9.00000E-08 P * T + 8.87500E-06 P * D + 3.68750E-06 P * F - 0.000012 T * D + 0.000011 T * F$$

$$+ 0.000659 D * F + 4.24844E-07 P^2 + 1.21562E-06 T^2 + 0.000286 D^2 + 0.000903 F^2\}$$

The equation in terms of actual factors can be used to make predictions about the response for given levels of each factor. Here, the levels should be specified in the original units for each factor. This equation should not be used to determine the relative impact of each factor because the co-efficient are scaled to accommodate the units of each factor and the intercept is not at the center of the design space. The adequacy of the above relation is tested by analysis of variance(ANOVA). The ANOVA test results are given in Table 4. at the desired confidence level of 95%. The relationship may be considered to be adequate. If the calculated value of the  $F_{ratio}$  of the developed relationship does not exceed the tabulated value of  $F_{ratio}$  for an anticipated level of confidence and the model is found to be adequate. The Fisher's F-test with a very low probability value demonstrates a very high significance of the regression model. The goodness of fit of the model is fitted by the determination co-efficient ( $R^2$ ). The coefficient of determination was calculated to be 0.985 in response which implies that 98.5% of the experimental values confirm the compatibility with data as predicted by the model. The  $R^2$  value should always be between 0 and 1. A model is statistically good the  $R^2$  value should be close to 1.0. Then adjusted  $R^2$  value reconstructs the expression with the significant terms. The Model F-value of 73.01 implies the model is significant. There is only a 0.01% chance that an F-value this large could occur due to noise-values less than 0.0500 indicate model terms are significant. In this case P, T, D, F, PD, PF, TF, DF,  $P^2$ ,  $T^2$ ,  $F^2$  are significant model terms. Values greater than 0.1000 indicate the model terms are



not significant. If there are many insignificant model terms (not counting those required to support hierarchy), model reduction may improve the model. The Lack of Fit F-value of 0.72 implies the Lack of Fit is not significant relative to the pure error. Non-significant lack of fit is good hence the model is considered to be fit. The value of adj.  $R^2=0.97$  is also high and indicates the high significance of the model. The pred.  $R^2$  value is 0.94 which means that the model could explain 94% of the variability in prediction. Adequate measures of the signal to noise ratio, a ratio greater than 4 is desirable. During this investigation the ratio is 29.36, which indicates an adequate signal. The model can be used to navigate the design space.

#### IV. OPTIMIZING THE LASER PARAMETERS

The surface and contour plots are shown in Figure 4 (A–F) for each process parameters. From the Response surface and contour plots graphs, it can be observed that when the Wear Rate trends to decrease with increasing Powder Feed Rate. It may be validated due to increase in hardness of laser hardfaced surface. The Wear Rate increases with increasing laser power because the high heat input will rise the depth of penetration and increases the rate of dilution of the deposits. Contour plot shows a vital role in the erudition of the response surface. It is clear that the Wear Rate get minimized with the rise in powder feed rate (F) and defocusing distance (D). With an increase of process parameters such as laser power (P) and travel speed (T), the wear rate reaches to a minimum level and then it starts to

multiply. Wear Rate mainly depends on dilution, hardness and microstructure. When the powder feed rate increases the dilution rate is minimized which because of more amount of heat is utilized for melting the hardfacing powder material and only a very small amount of heat is enough to melt the substrate material. So that the hardness of the hardfaced surface increases and leads to the decrease in Wear Rate. The rate of dilution reduces with the increase of defocusing distance which leads the decrease of wear rate to certain limit. With increasing the Transfer speed, the powder density per square area becomes less hence there is an upturn in the dilution rate and it rise the value of Wear Rate. Laser power is mainly used for melting the powder but when it keeps increasing, the high volume of substrate material begins to melts which leads to the results of an upturn in dilution, as the variation of Wear Rate in laser hardfaced sample could be affected by the dilution. As the results of higher dilution the hardness of laser hardfaced sample falls down which leads to an increasement in wear rate. So the dilution should be kept minimum to attain the achievable minimum wear rate. Increasing Laser Power raises the dilution rate and multiplies the Wear Rate. By analysing the response surface and contour plots as shown in Figure 4 (A–F), the optimized rounded values of laser hardfacing parameters are shown in Table.6. It is found that the minimum wear rate of 0.155388 (mg/N-km) can be achieved by the laser power of 2615 (W), Travel speed of 634 (mm/min), Defocusing distance of 22 (mm) and Powder feed rate of 12.5 (g/min).

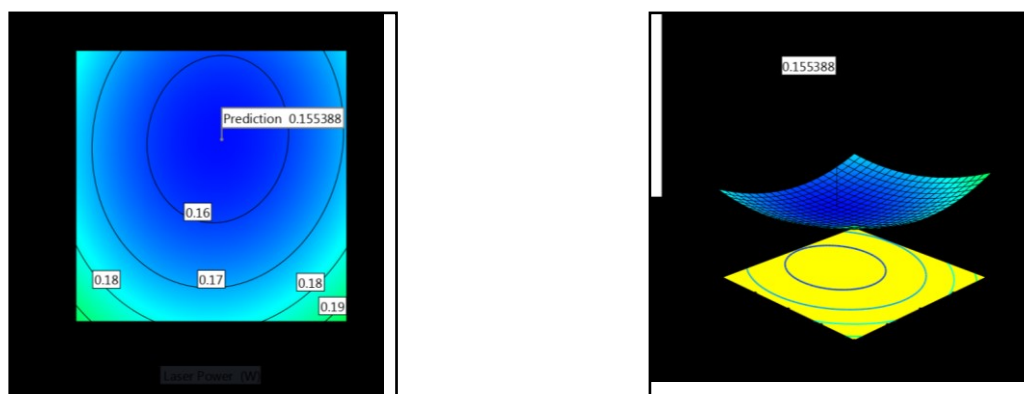


Figure 4 A: Interaction effect of Laser Power and Travel Speed

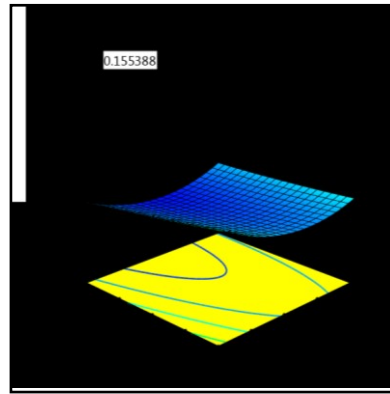
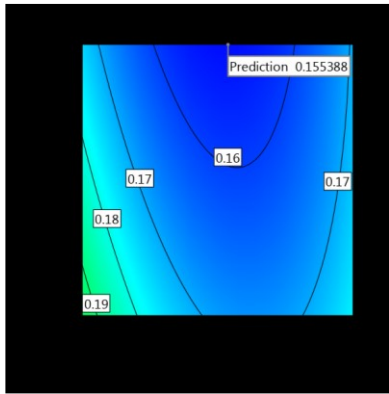


Figure 4 B: Interaction effect of Laser Power and Defocusing Distance

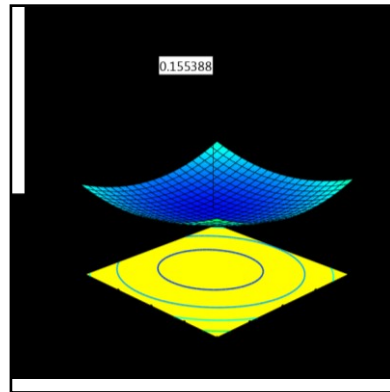
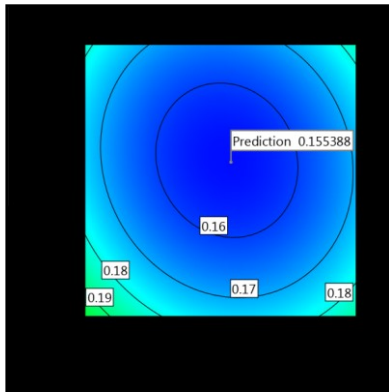


Figure 4 C: Interaction effect of Laser Power and Powder Feed Rate

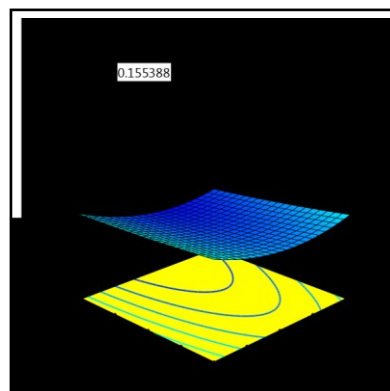
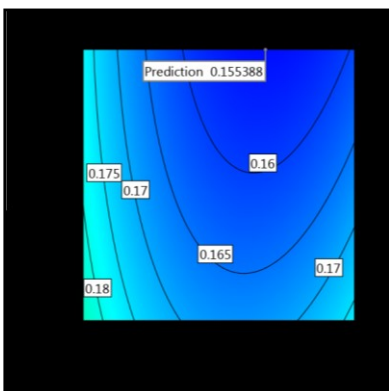


Figure 4 D: Interaction effect of Travel Speed and Defocusing Distance

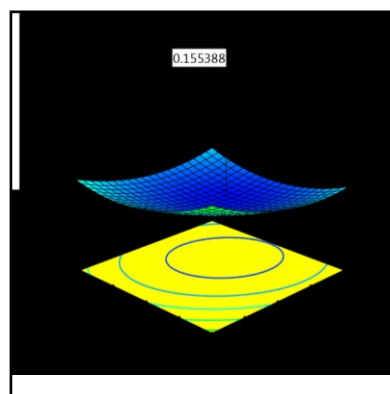
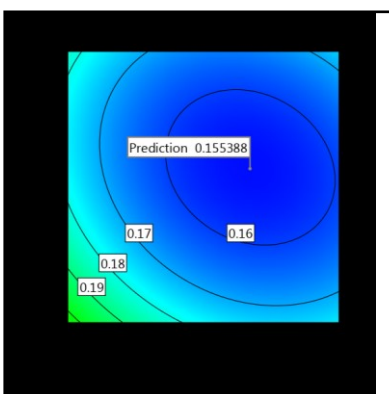


Figure 4 E: Interaction effect of Travel Speed and Powder Feed Rate.

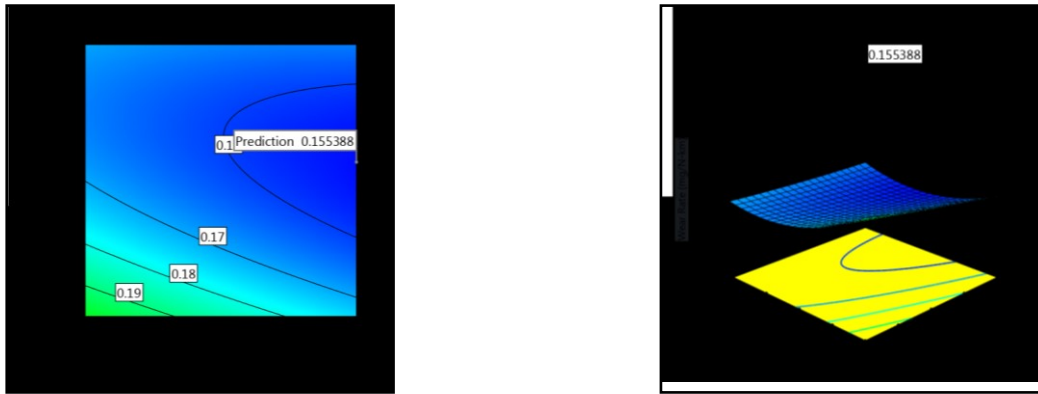


Figure 4 F: Interaction effect of Powder Feed Rate and Defocusing Distance

S. No	Important Laser Parameters	Optimized Value
1	Laser Power (P)	2615 (W)
2	Travel Speed (T)	634 (mm/min)
3	Defocusing Distance (D)	22 (mm)
4	Powder Feed Rate (F)	12.5 (g/min)

Table 6: Optimized Hardfacing Parameters for wear rate.

## V. CONCLUSION

An empirical relationship was developed to predict the Wear Rate of cobalt-based (Stellite-6) hardfaced layer produced on AISI 304 Stainless-Steel substrates by incorporating important Laser Hardfacing parameters such as Laser power(P), Travel speed (T), Defocusing distance (D), and Powder feed rate (F). A minimum Wear Rate of 0.155388 (mg/N-km) could be achieved in the Laser hardfaced surface which was produced by the Laser Power of 2615 (W), Travel Speed of 634 (mm/min), defocusing distance of 22 (mm) and Powder Feed Rate of 12.5 (g/min). The Powder Feed Rate is identified as the major influencing factor than other three laser hardfacing parameters to predict the Wear Rate of Hardfaced surfaces.

## VI. REFERENCES

- [1]. P. Balu, P. Leggett, "Multi-response optimization of laser-based powder deposition of multi-track single layer hastelloy C-276," *Mater. Manuf. Process.*, vol. 28, no. 2, pp. 173–182, (2013).
- [2]. K. Y. Benyounis "Optimization of different welding processes using statistical and numerical approaches - A reference guide," *Adv. Eng. Software.*, vol. 39, no. 6, pp. 483–496, (2008).
- [3]. S. Guo, Z. Chen, D. Cai, and J. Yao, "Prediction of simulating and experiments for co-based alloy laser cladding by HPDL," *Phys. Procedia*, vol. 50, no. October 2012, pp. 375–382, (2013).
- [4]. M. K. Alam, N. Nazemi, "Investigating Process Parameters and Microhardness Predictive Modeling Approaches for Single Bead 420 Stainless Steel Laser Cladding," August, (2017).
- [5]. Wood, P. D, Evans, H. E. and Ponton, C. B. "Investigation into the wear behaviour of Stellite 6 during rotation as an unlubricated bearing at 600 °C", *Tribology. Int.* 44, pp. 1589–1597 (2011).
- [6]. Luo., H. li. "Abrasive Wear Comparison of Cr<sub>3</sub>C<sub>2</sub>/Ni<sub>3</sub>Al Composite and Stellite 12 Alloy Cladding". *J. Iron Steel Res. Int.* 14, pp. 15–20, (2007).
- [7]. S. Liu., "Statistical analysis and optimization of processing parameters in high-power direct diode laser cladding," *Int. J. Adv. Manuf. Technol.*, vol. 74, no. 5–8, pp. 867–878, (2014).
- [8]. F. Madadi, F. Ashrafzadeh, "Optimization of pulsed TIG cladding process of stellite alloy on carbon steel using RSM," *J. Alloys Compd.*, vol. 510, no. 1, pp. 71–77, (2011).
- [9]. B. R. Moharana, "Experimental investigation on mechanical properties of AISI 304 to Cu joints by



- CO<sub>2</sub> laser,” *Eng. Sci. Technol.Int. J.*, vol. 19, no. 2, pp. 684–690, (2016).
- [10]. I. Tabernero, A. Calleja, A. Lamikiz, and L. N. López De Lacalle, “Optimal parameters for 5-axis Laser cladding,” *Procedia Eng.*, vol. 63, pp.45–52, (2013).
- [11]. Ahn, D. G. “Hardfacing technologies for improvement of wear characteristics of hot working tools”: A review. *Int. J. Precis. Eng. Manuf.* pp. 14, pp. 1271–1283, (2013).
- [12]. Ameen, H. “Effect of loads, sliding speeds and times on the wear rate for different materials”. *Am.J. Sci. Ind. Res.* 2, pp. 99–106 (2011).
- [13]. K. S. H. Prasad, C. S. Rao, “Application of Design of Experiments to Plasma Arc Welding Process: A Review,” *J. Brazilian Soc. Mech. Sci. Eng.*, vol. 34, no. 1, pp. 75–81, (2012).
- [14]. Liu, R., Yao, J. H., Zhang, Q. L., Yao, M. X. and Collier, R. Sliding wear and solid- particle erosion resistance of a novel high-tungsten Stellite alloy. *Wear* 322–323, pp. 41–50, (2015).
- [15]. Motallebzadeh, A., Atar, E. and Cimenoglu, H. Sliding wear characteristics of molybdenum containing Stellite 12 coating at elevated temperatures. *Tribology. Int.* 91, pp. 40–47, (2015).